Numerical investigation on behaviour of ablation arcs confined with different polymer materials

NUMERICAL INVESTIGATION ON BEHAVIOUR OF ABLATION ARCS CONFINED WITH DIFFERENT POLYMER MATERIALS

Y Tanaka[1], K Kawasaki[1], T Onchi[1,2], Y Uesugi[1]

[1]Div. of Electrical Eng. & Computer Sci., Kanazawa Univ., JAPAN. tanaka@ec.t.kanazawa-u.ac.jp
[2]Fuji Electric Advanced Technology Co. Ltd, JAPAN.

ABSTRACT

Numerical simulation was made for an arc plasma confined with different polymer materials to investigate influence of polymer ablation on the behavior of the arc plasma. Polymer ablation phenomena are nowadays crucial for the interruption ability of downsized low-voltage and high-voltage circuit breaker design. In this work, a two-dimensional thermofluid model of an arc plasma was developed taking account of mass and energy exchanges due to polymer ablation without empirical parameters. Using this model, we calculated influence of ablation on the gas flow and temperature fields for different polymer materials. The resultant arc voltage was also compared among different polymer materials.

1. INTRODUCTION

Understanding of the polymer ablation phenomena is nowadays greatly important for downsized circuit breaker design [1]–[5]. For example, a polymer-ablation assisted type of the low-voltage molded case circuit breaker (MCCB) has been developed [6], and a prototype of polymer-ablation assisted high-voltage gas circuit breaker has been tested [7]. These circuit breakers utilize polymer ablation to raise the pressure in the chamber, which involves producing strong gas flow or increasing the arc voltage. However, the polymer ablation phenomena are very complicated including the mass and energy exchanges between the polymer solid and the plasma, phase transition, pressure rise, etc. In addition, properties of the polymer ablated vapor may markedly affect the interruption ability of the circuit breakers. Such complication of polymer ablation phenomena makes it difficult to sufficiently understand.

In this paper, a two-dimensional thermofluid model was developed for an arc plasma confined by polymer wall considering mass and energy exchange due to the polymer ablation. Polytetrafluoroethlene (PTFE), polymethylmethacrylate (PMMA), polymethylene (POM), and polyamide-66 (PA66) were treated in this work. The gas flow and temperature fields were computed by taking account of the ablated vapor properties. Results show that the PA66 and PMMA ablation increases the arc voltage more than PTFE and PE because of the lower electrical conductivity of their ablated vapors.

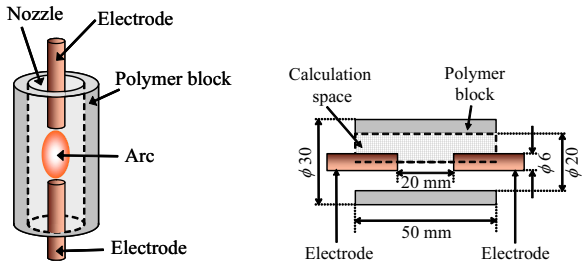

(a) Arc model. (b) Calculation space.

Fig. 1. Arc model and calculation space.

2. MODELLING

2.1. Calculation model and calculation space

Fig. 1(a) illustrates the schematic diagram of the calculation model in this work, and Fig.1(b) shows the calculation space. An arc plasma is assumed to form between two simple cylindrical electrodes. The diameter of the electrodes is 6.0 mmϕ. The distance between the electrodes is set to 20 mm. Around the arc plasma and the electrodes, a cylindrical polymer tube is located. Its inner diameter is 20 mmϕ. If the arc plasma contacts the polymer wall, the wall is ablated to contaminate the arc plasma with ablated polymer vapor. For simulating such an arc plasma with polymer ablation, a two-dimensional cross section indicated in Fig. 1(b) was adopted.

In this paper, the followings are assumed: (i) local thermodynamic equilibrium condition is established in the arc plasma, (ii) the gas flow is laminar, (iii) interactions between the electrode and the arc plasma, including evaporation and electron emission, were neglected for simplicity, (iv) initially space between the electrode is filled with pure air.

2.2. Governing equations

In accordance with the assumptions in the previous section, the arc plasma is governed by the following equations:

-Mass conservation:

$$\frac{\partial \rho}{\partial t} + \nabla \cdot (\rho \boldsymbol{u}) = S_{\mathrm{p}}^{C} \tag{1}$$

-Momentum conservation:

$$\frac{\partial (\rho \boldsymbol{u})}{\partial t} + \nabla \cdot (\rho \boldsymbol{u}\boldsymbol{u}) =$$

$$-\nabla p + \nabla\boldsymbol{\tau} + \sigma\mu_0(\boldsymbol{E}\times\boldsymbol{H}) \quad (2)$$

-Energy conservation:

$$\frac{\partial(\rho h)}{\partial t} + \nabla\cdot(\rho\boldsymbol{u}h) = \nabla\cdot(\frac{\lambda}{C_\mathrm{p}}\nabla h) + \frac{\partial p}{\partial t} + \sigma|\boldsymbol{E}|^2 - P_\mathrm{rad} - LS_\mathrm{p}^C \quad (3)$$

-Mass conservation of polymer vapor:

$$\frac{\partial(\rho c_\mathrm{pol})}{\partial t} + \nabla\cdot(\rho\boldsymbol{u}c_\mathrm{pol}) = \nabla\cdot(\rho D_\mathrm{pol}\nabla c_\mathrm{pol}) + S_\mathrm{p}^C \quad (4)$$

where t: the time, $\boldsymbol{u}$: the gas flow vector, ρ: the mass density, S_p^C: the mass production rate due to ablation, p: the pressure, $\boldsymbol{\tau}$: the stress tensor, $\boldsymbol{E}$: the electric field vector, $\boldsymbol{H}$: the magnetic field vector, μ_0: the permeability of vacuum, σ: the electrical conductivity, h: the enthalpy, λ: the thermal conductivity, C_p: the specific heat, P_rad: the radiation loss, L: the latent heat for polymer ablation, c_pol: the mass fraction of polymer ablated vapor, D_pol: the effective diffusion coefficient of polymer vapor against air. In addition, we assumed that the electric field and magnetic field have only axial and azimuthal components, respectively, that is, $\boldsymbol{E} = (0, 0, E_z)$ and $\boldsymbol{H} = (0, H_\theta, 0)$. In this case, the electric field strength and magnetic field strength can be calculated from:

-Ohm's law:

$$E_\mathrm{z} = \frac{I}{\int_0^\infty 2\pi\sigma r dr} \quad (5)$$

-Ampere's law:

$$H_\theta = \frac{1}{r}\int_0^r \sigma E_z \xi d\xi \quad (6)$$

where I is the total electric current.

The total electric current I was set to 100 $\mathrm{A_{dc}}$ for a fundamental study of polymer ablation arcs in this work.

2.3. Mass production rate due to ablation

The mass production rate due to ablation S_p^C was approximately calculated as follows:

$$S_\mathrm{p}^C = \begin{cases} m_\mathrm{pol}(\Gamma_\mathrm{ab} - \Gamma_\mathrm{dep})\dfrac{\Delta S}{\Delta V} & \\ \qquad\text{(neighbor to wall)} & \\ 0 \qquad\text{(otherwise)} & \end{cases} \quad (7)$$

where m_pol is the effective mass of polymer ablated vapor, Γ_ab is the ablation flux from the solid polymer surface, Γ_dep is the deposition flux onto the solid polymer surface, ΔS is the surface area of the ablated wall in a calculation cell, ΔV is the volume of a calculation cell. The ablation flux Γ_ab was calculated by the following Hertz-Knudsen relation [8]:

$$\Gamma_\mathrm{ab} = \frac{P_\mathrm{v}}{\sqrt{2\pi m_\mathrm{pol} kT}} \quad (8)$$

where P_v is the saturation vapor pressure of polymer ablated vapor, k is Boltzmann constant, T is the temperature. The saturation vapor pressure P_v at temperatures above the melting temperature was evaluated using the Clausius-Clapeyron's relation [9]:

$$\frac{dP_\mathrm{v}}{dT} = \frac{L}{R_\mathrm{pol}T^2}P_\mathrm{v} \quad (9)$$

where R_pol is the gas constant of the polymer vapor. On the other hand, the deposition flux Γ_dep was calculated from the random flux:

$$\Gamma_\mathrm{dep} = \frac{1}{4}\frac{\rho c_\mathrm{pol}}{m_\mathrm{pol}}\overline{v} = \rho\left(\frac{kT}{2\pi m_\mathrm{pol}^3}\right)^{\frac{1}{2}} c_\mathrm{pol}. \quad (10)$$

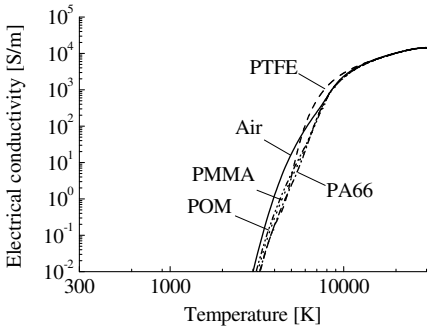

Fig. 2. Electrical conductivity of different polymer ablated vapors and air.

2.4. Thermodynamic properties of solid polymer and transport properties of ablated vapor

Thermodynamic properties of solid PTFE, PMMA, PA66, and POM were actually measured using the thermogravimetry differential thermal analysis (TG-DTA) and the differential scanning calorimetry (DSC) method. Table I summarizes the measured thermodynamic properties of solid polymer. These properties were used in the present numerical simulation.

Thermodynamic and transport properties such as ρ, h, C_p, m_pol, R_pol, λ, σ and viscosity μ of polymer ablated vapor were calculated using the computed equilibrium composition and the collision integrals between species. The first approximation of Chapman-Enskog method was used for calculation of the transport properties [10]. Fig. 2 shows the calculated electrical conductivity of polymer ablated vapors and air. As seen, PA66 ablated vapor has the lowest σ, whilst POM ablated vapor has the highest σ at temperatures 3000–5000 K among the polymer materials treated here. This is because POM vapor has much CHO molecules at this temperature range, which are important electron suppliers with the lowest ionization potential among species in ablated vapor.

3. RESULTS AND DISCUSSIONS

3.1. Gas flow and temperature fields

Figs. 3(a) and 3(b) show the gas flow field in arc plasmas confined by PTFE and PMMA walls as examples. The gas flow is produced from the polymer wall to

Table I. Thermodynamic properties of polymers.

	PTFE	PMMA	POM	PA66
Mass density [kg/m^3]	2160	1163	1410	1140
Melting temperature [K]	618	–	435	536
Boiling/thermal decomposition temperature [K]	809	618	605	669
Latent heat for melting [kJ/kg]	50.4	–	123	62
Latent heat for evaporation [kJ/kg]	936.7	251.6	1022	222
Specific heat of solid [J/kg/K]	1035	1779	1983	2036
Specific heat of liquid [J/kg/K]	1419	1919	2099	3031

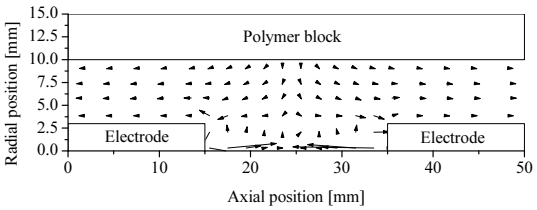

(a) PTFE.

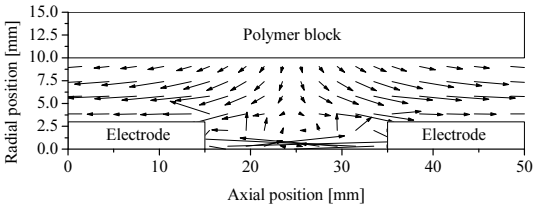

(b) PMMA.

Fig. 3. Gas flow field in arc plasmas confined by PTFE and PMMA walls.

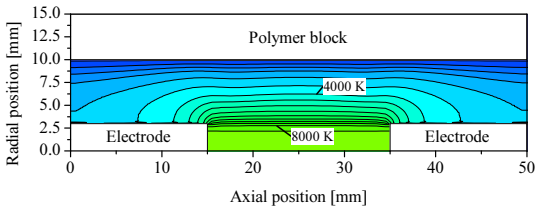

(a) PTFE.

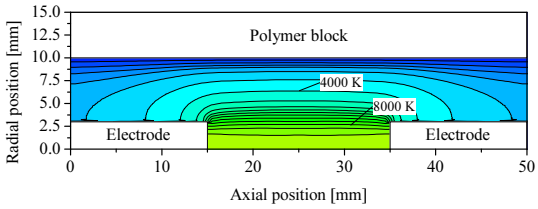

(b) PMMA.

Fig. 4. Temperature flow field in arc plasmas confined by PTFE and PMMA walls.

the arc plasma in the radial direction. In PMMA case, the stronger radial gas flow is created to shrink the arc plasma than in PTFE case. This radial gas flow is formed from pressure rise near the surface wall due to the polymer wall ablation. For POM and PA66 cases, stronger radial gas flow was also created than for PTFE case.

The temperature distributions in arc plasmas confined by the PTFE and PMMA walls were also calculated as indicated in Figs. 4(a) and 4(b). These figures depict that the temperature near the polymer wall decreases to 600–700 K. This temperature decline near the polymer wall may be attributable to the energy consumption for polymer wall ablation. This lower temperature is transferred by the strong radial gas flow, which results in the shrinkage of the arc plasma.

Similar calculations were made for different polymer walls such as PTFE, PMMA, POM, and PA66. Fig. 5 indicates the radial temperature distributions at an axial position of 25 mm in arcs confined by different polymer walls. The radial temperature distribution of an air arc without polymer ablation is also added in these figures for comparison. For this simulation of an air arc, the wall is assumed to be adiabatic without ablation. As seen in this figure, the air arc without polymer ablation has temperatures above 7000 K even near the wall. On the other hand, the polymer ablated arcs have much lower temperatures than the air arc. In particular, the temperature near the polymer wall is remarkably decreased to 600–700 K for any polymer walls, and then the high radial gradient of the temperature is produced. However, little difference can be found in the temperature distributions among the different polymer materials.

3.2. Arc voltage and energy loss due to ablation

For the low-voltage circuit breaker, the arc voltage is one of the important parameters because the arc voltage should be raised to higher value than the electric power source voltage for the current interruption. The arc

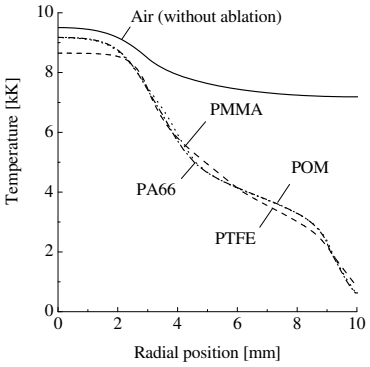

Fig. 5. Radial temperature distributions in arc plasmas confined by polymers.

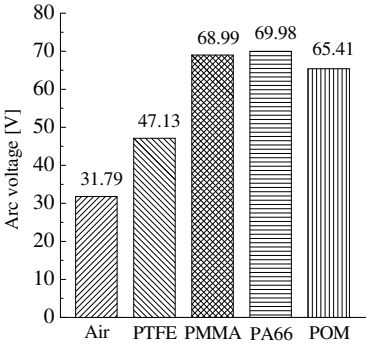

Fig. 6. Arc voltage for different polymer ablated arcs.

voltage is influenced by the polymer ablation phenomena including mixing of polymer ablated vapor with air, and also by the resultant gas flow and temperature in the arc plasma. Fig. 6 indicates the calculated arc voltage for different polymers. The arc voltage was calculated by integrating the electric field between the electrodes. In the air arc without ablation, the arc voltage is only 32 V. However, the polymer ablation arcs have much higher arc voltages than the above value. For example, the PMMA ablated arc has the arc voltage about 69 V which is twice higher than that of the air arc. Among the polymer materials adopted here, the PA66 ablated arc has the highest arc voltage, while the PTFE ablated arc does the lowest arc voltage. The difference in the arc voltage for different polymer materials is mainly attributed to the electrical conductivity of polymer ablated vapor under the present calculation condition. The PA66 has a lower electrical conductivity at given temperatures below 10000 K as indicated in Fig. 2, which results in the higher arc voltage.

This model can estimate the mass loss rate $\dot{m}_{\mathrm{abl}}$ of solid polymers and the power loss P_{abl} due to ablation. These were calculated by the following equation:

$$\dot{m}_{\mathrm{abl}} = 2\pi \iint S_{\mathrm{p}}^{C} r dr dz, \tag{11}$$

$$P_{\mathrm{abl}} = L \cdot \dot{m}_{\mathrm{abl}}. \tag{12}$$

Figs. 7(a) and 7(b) show $\dot{m}_{\mathrm{abl}}$ and P_{abl}, respectively, for

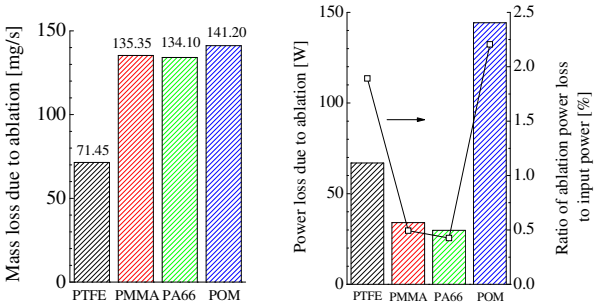

(a) Mass loss due to ablation.

(b) Radial temperature distribution.

Fig. 7. Mass loss and power loss due to ablation.

different polymer materials. The ratio of the ablation power loss to the total input power to the arc is also plotted in Fig. 7(b). As seen in these figures, it is predicted that the highest $\dot{m}_{\mathrm{abl}}$ and highest P_{abl} occurs in the POM ablation arc. This means that the arc temperature is more easily influenced in the POM ablation arc.

4. CONCLUSIONS

A two-dimensional thermofluid model was developed for an arc plasma confined by the polymer materials. Mass and energy exchanges due to the polymer ablation were considered in this model. Ablation rate was calculated using thermodynamic properties of solid polymer without empirical parameters. The gas flow and temperature fields were calculated in arc plasmas confined by PTFE, PMMA, PA66 and POM. As a result, we found that PA66 ablation causes the highest arc voltage because of its lowest electrical conductivity at temperatures 3000–5000 K compared to the other polymer materials. On the other hand, POM ablation produces a strong gas flow and requires higher power loss for ablation. These fundamental results will be helpful to understand the ablation arc phenomena.

References

[1] P Andre, *J. Phys. D: Appl. Phys.*, **30**, 475–93, 1997.

[2] P Chevrier, et al, *J. Phys. D: Appl. Phys.* **30** 1346–55, 1997.

[3] T Nielsen, et al, *J. Phys. D: Appl. Phys.*, **34**, 2022–31, 2001.

[4] M Seeger, et al, *J. Phys. D: Appl. Phys.* **39** 5016–24, 2006.

[5] R Kozakov, et al, *J. Phys. D: Appl. Phys.* **40** 2499–506, 2007.

[6] M Tsukima, et al, *Trans. IEEJ* **122-PE** 969–75, 2002 (in Japanese).

[7] T Uchii, et al, *Trans. IEEJ*, **124-PE**, 476–84, 2004 (in Japanese).

[8] M Knudsen, *Ann. Phys., Lpz.*, **47**, 697–708, 1915.

[9] W Kenneth, "Generalized Thermodynamic Relationships", Thermodynamics, 5th (in English), 1988, New York, McGraw-Hill.

[10] Y Tanaka, et al, *JSME Int. J.*, Ser. B, **48**, 417–24, 2005.